Thin Solid Films 636 (2017) 188–192

Contents lists available at ScienceDirect

Thin Solid Films

journal homepage: www.elsevier.com/locate/tsf

High energy storage responses in all-oxide epitaxial relaxor ferroelectric thin films with the coexistence of relaxor and antiferroelectric-like behaviors

Chi T.Q. Nguyen [a], Minh D. Nguyen [a,b,c,*], Hien T. Vu [a], Evert P. Houwman [b], Hung N. Vu [a], Guus Rijnders [b]

[a] International Training Institute for Materials Science (ITIMS), Hanoi University of Science and Technology, No. 1 Dai Co Viet road, Hanoi 10000, Vietnam
[b] MESA + Institute for Nanotechnology, University of Twente, P.O. Box 217, 7500AE Enschede, The Netherlands
[c] Solmates B.V., Drienerlolaan 5, 7522NB Enschede, The Netherlands

ARTICLE INFO

Article history:
Received 12 February 2017
Received in revised form 8 May 2017
Accepted 1 June 2017
Available online 2 June 2017

Keywords:
Relaxor ferroelectrics
Epitaxial growth
Orientation
Energy storage

ABSTRACT

Relaxor ferroelectric $Pb_{0.9}La_{0.1}(Zr_{0.52}Ti_{0.48})O_3$ (PLZT) thin films have been epitaxially grown via pulsed laser deposition on $SrRuO_3/SrTiO_3$ single crystal with different orientations. The high recoverable energy-storage density and energy-storage efficiency in the epitaxial PLZT thin films are mainly caused by the coexistence of relaxor and antiferroelectric-like behaviors. The recoverable energy-storage density of 12.03, 12.51 and 12.74 J/cm^3 and energy-storage efficiency of 86.50, 88.14 and 88.44%, respectively, for the PLZT(001), PLZT(011) and PLZT(111) thin films measured at 1000 kV/cm. The high energy density and high efficiency indicate that the relaxor epitaxial PLZT(111) thin film is a promising candidate for high pulsed power capacitors.

1. Introduction

Dielectric materials with high energy-storage density and high efficiency are greatly needed for the potential application in advanced pulse power capacitors for electronics and electrical power systems [1]. Based on the physical principals, the materials with higher maximum polarization (P_{max}) and smaller remanent polarization (P_r) are the most promising candidates [2]. Ferroelectric materials have a relatively high P_r value, leading to low recoverable energy-storage density (U_{reco}) and energy-storage efficiency (η) [3,4]. Antiferroelectric materials have a low P_r, but also wide hysteresis loops, leading to large energy loss [5–8]. Relaxor ferroelectric materials exhibit slim polarization hysteresis loops with low P_r, suggesting higher U_{reco} and η values [1,9,10].

Recently, tuning the properties of lead zirconate titanate (PZT) from the normal ferroelectric to either relaxor ferroelectric or antiferroelectric phases by the doping effect has been reported. Previous studies indicated that the La^{3+} substitution for Pb^{2+} in PZT induces the distortion of the unit cells for easy of domain switching and decrease the oxygen vacancies, inducing a ferroelectric-to-relaxor transition [4,11]. We also indicated that the energy storage responses in the epitaxial relaxor $Pb_{0.9}La_{0.1}(Zr_{0.52}Ti_{0.48})O_3$ (PLZT) films grown on $SrRuO_3/SrTiO_3$/Si (U_{reco} = 13.7 J/cm^3 and η = 88.2% [1]) are significantly larger than for polycrystalline relaxor PLZT films on $Pt/Ti/SiO_2/Si$ (U_{reco} = 11.5 J/cm^3 and η = 52.5% [12]), due to the coexistence of relaxor ferroelectric and antiferroelectric phases in the epitaxial PLZT films. In this study, the orientation-dependent microstructure and energy storage performance of the relaxor epitaxial PLZT films deposited on $SrRuO_3/SrTiO_3$ substrates have been investigated.

2. Experimental procedure

In this paper, $Pb(Zr_{0.52}Ti_{0.48})O_3$ (PZT) and $Pb_{0.9}La_{0.1}(Zr_{0.52}Ti_{0.48})O_3$ (PLZT) thin films were deposited on $SrRuO_3/SrTiO_3$ (SRO/STO) substrates with different orientations using a pulsed laser deposition (PLD) method. The morphotropic phase boundary composition was based on the results of Hu et al. [13]. The optimized deposition conditions of the PZT and PLZT thin films were: laser repetition rate 10 Hz, energy density 2.5 J/cm^2, oxygen pressure 10 Pa and substrate temperature 600 °C [14]. For the top and bottom SRO electrodes the conditions were: laser repetition rate 4 Hz, energy density 2.5 J/cm^2, oxygen pressure 13 Pa and substrate temperature 600 °C. The thicknesses of the top and bottom SRO electrodes are about 100 nm.

Crystallographic properties of the thin films were analyzed by X-ray θ-2θ scans (XRD) and omega scans using a PANalytical X-ray diffractometer with Cu-$K\alpha$ radiation (wavelength: 1.5405 Å). Normal operating power is 1.8 kW (45 kV and 40 mA). Atomic force microscopy (AFM:

* Corresponding author at: International Training Institute for Materials Science (ITIMS), Hanoi University of Science and Technology, No. 1 Dai Co Viet Road, Hanoi 10000, Vietnam.
E-mail address: minh.nguyen@itims.edu.vn (M.D. Nguyen).

http://dx.doi.org/10.1016/j.tsf.2017.06.003
0040-6090/

Bruker Dimension Icon) and cross-sectional high-resolution scanning electron microscopy (HRSEM: Zeiss-1550) were performed to investigate the morphology, microstructure and thickness of the as grown thin films. For electrical measurements, 100 × 100 μm^2 capacitors were patterned with a standard photolithography process and structured by argon-beam etching of the top-electrodes and wet-etching (*HF-HCl* solution) of the PZT and PLZT films. The polarization hysteresis loop measurements were performed with the ferroelectric mode of the aixACCT TF-2000 Analyzer at 1 kHz and ± 200 kV/cm amplitude. A Süss MicroTech PM300 manual probe station equipped with a Keithley 4200 Semiconductor Characterization System was used for the capacitance measurement. The capacitance-electric field (*C-E*) curves were measured up to a *dc*-electric field of ± 200 kV/cm and with a 1 kHz frequency *ac*-electric field with 3.3 kV/cm amplitude. The corresponding dielectric constants were calculated from the *C-E* curves. All measurements were performed at room temperature.

3. Results and discussion

Crystalline structure of the PLZT thin films was investigated using X-ray diffraction (XRD) measurements. Fig. 1(a–c) shows the XRD patterns of the PLZT films deposited on SRO/STO substrates with different orientations. All the films are strong preferred orientation and have a pure perovskite phase. Apparently, the PLZT film on the STO (001) substrate shows a strong (001) orientation, while the PLZT films on STO (011) and STO (111) substrates display (011) and (111) orientations, respectively. In addition, the full-width at half-maximum values obtained from the rocking curves of the PLZT films, as indicated in Fig. 1d, are 0.12°, 0.31° and 0.56° for (001)-, (011)-, (111)-oriented PLZT films, respectively. Such narrowness of the three peaks represents the films with the high single crystalline quality from epitaxial growth.

The surface morphology and roughness of PLZT films have been measured by AFM, as shown in Fig. 2(a–c). The root-mean square surface roughness is about 1.15, 4.81 and 6.66 nm for the PLZT deposited on STO (001), STO (011) and STO (111) substrates, respectively. The change in the surface roughness can be explained by the difference in the microstructure from the compact and dense structure in the PLZT(001) film to the bar-columnar and grain-columnar structures in the PLZT(011) and PLZT(111) films (Fig. 2(d–f)), respectively, and it can be explained by the change in the corresponding schematic diagram of the unit cells (Fig. 2(g–i)). The columnar structure is a reason to increase the film thickness of 526 and 503 nm, respectively, in the PZT(111) and PZT(011) films, in comparison with the film thickness of 482 nm in the PZT(001) film.

Metal-ferroelectric-metal capacitors containing relaxor PLZT thin films with varying orientation were electrically characterized using polarization-electric field (*P–E*) measurements, which were indicated in Fig. 3(a–c). All the relaxor films exhibit double loops, demonstrating their antiferroelectric (AFE)-like behaviors. In order to get the better significance of AFE-like behavior in relaxor PLZT thin films, the switching current and capacitance curves were also investigated (Fig. 4). It is indicated that the double-butterfly-shaped *C-E* curves and four switching peaks in the switching current measurements were detected for these films. On the other hand, the AFE-like behavior is observed in these relaxor films. Moreover, the AFE-like behavior in the PZT(001) thin film is more dominant than that in the PZT(011) and PZT(111) thin films due to the sharper peak in the switching current of the PZT(001) thin film, as shown in Fig. 4(a–c).

The transition from normal relaxor ferroelectric with slim 'single' hysteresis loop (or two peaks in switching current curve) [12,15] to antiferroelectric-like characteristics is observed in the relaxor PLZT thin films grown on SRO/STO substrates. The AFE-like behavior appears to be related to the crystalline quality of the bottom SRO/PLZT interface. In analogy with previous experiments with the growth of thin PZT layers on SRO/STO [16], where the SRO grows epitaxially strained to the (relaxed) STO, adopting its in-plane lattice parameter. The initial growth layer of the PLZT starts to grow epitaxially compressively strained to the SRO/STO, but relaxes within a few nm (possibly up to about 10 nm as in ref. [16]) to its bulk value, by defect incorporation. It is indicated that the compressive-in-plane strain induces an AFE state in the initial growth layer, while the largest, relaxed part of the film has the normal relaxor behavior. The AFE-like behavior is also found in the relaxor PLZT films grown on SRO/STO/Si but not on SRO/CeO_2/YSZ/Si substrate, due to the higher degree single crystalline with initial lattice matching at the SRO bottom electrode [1]. This explanation suggests that the induced AFE layer is present at the bottom electrode interface, while the remainder of the film is in the relaxor phase.

Previous studies have also indicated that the shape of the *P-E* loop becomes slimmer and slanted with increasing La concentration in the PZT films [4]. This is attributed to the reduction of the tetragonality of

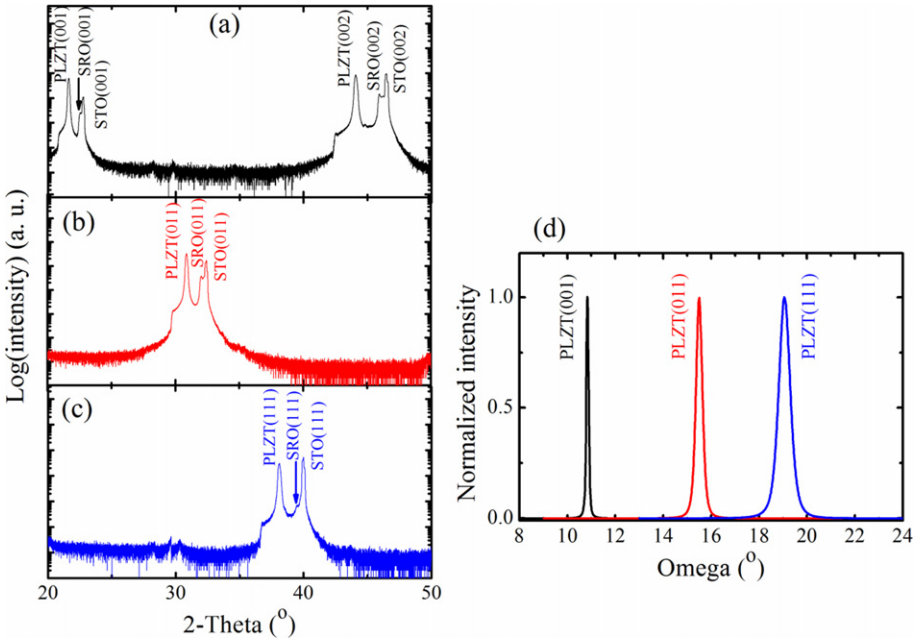

Fig. 1. XRD pattern of θ–2θ scans for the PLZT films deposited on (a) STO (001), (b) STO (011) and (c) STO (111); (d) the corresponding rocking curves of these films.

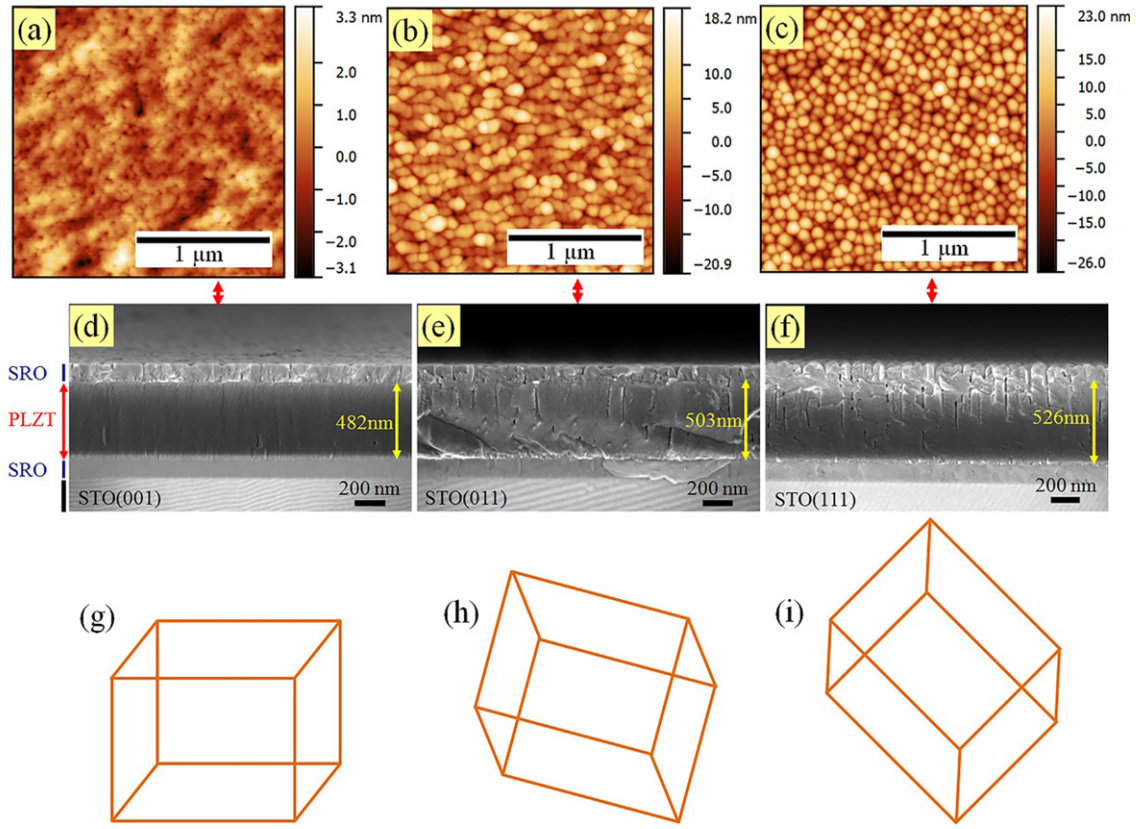

Fig. 2. Surface AFM morphology images of the (a) PLZT(001), (b) PLZT(011) and (c) PLZT(111) films; (d–f) the corresponding cross-sectional SEM images; (g–i) the corresponding schematic diagram of the unit cells.

the PLZT unit cell with increasing La content, leading to a decrease in spontaneous polarization in the unit cell [17]. Therefore, the polarizations in the PLZT films in this study are found to be much lower than those in the corresponding PZT films (Fig. 5a). As expected, the remanent polarization changed with the PZT film orientation, with (001)- and (111)-oriented films having the largest and smallest values, while all films have the similar maximum polarization. Moreover, the (001)-oriented film exhibits nearly square hysteresis loop with sharp electric field switching, whereas the (011)- and (111)-oriented films indicate more slanted hysteresis loops.

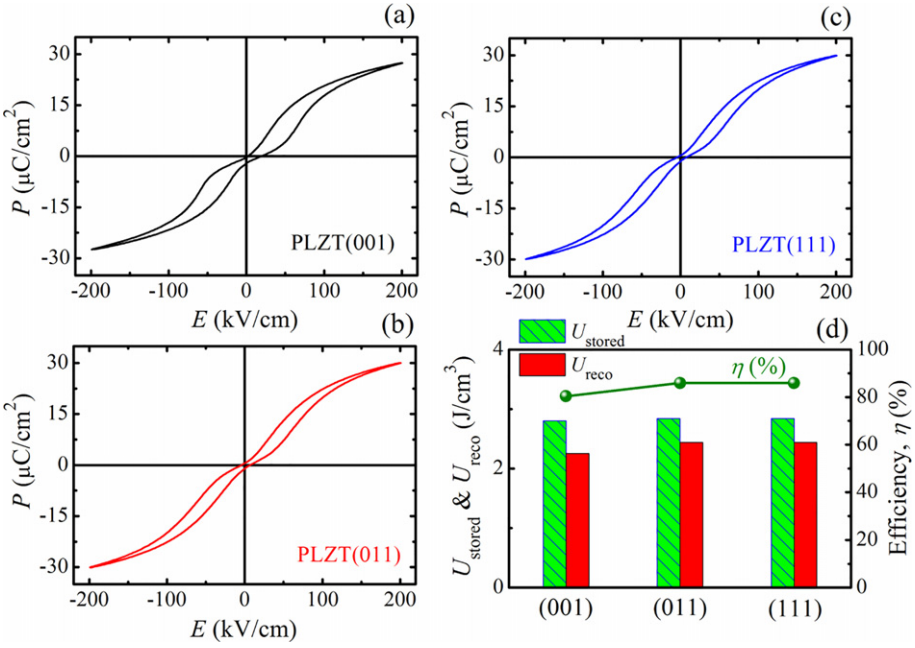

Fig. 3. Ferroelectric hysteresis (P–E) loops of the (a) PLZT(001), (b) PLZT(011) and (c) PZT(111) thin films; (d) The corresponding energy-stored per unit volume (U_{stored}), recoverable energy-storage density (U_{reco}) and energy-storage efficiency (η) of the thin films. The measurements were performed at ±200 kV/cm and 1 kHz frequency.

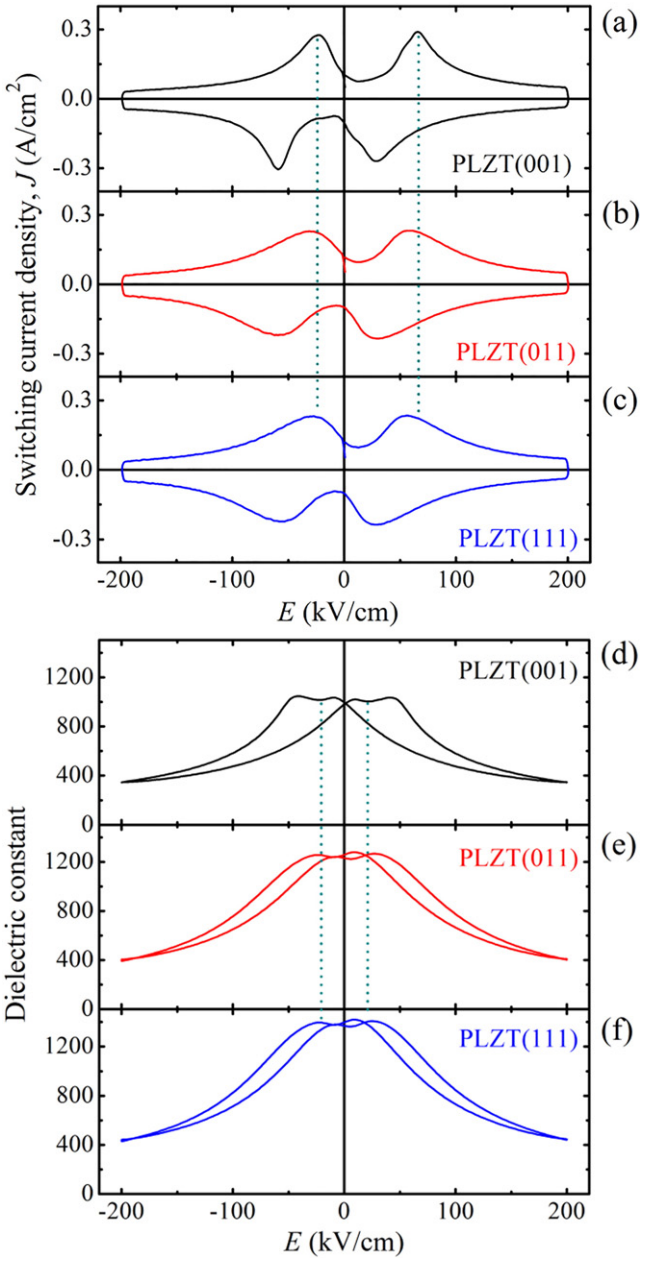

Fig. 4. (a–c) Switching current (J–E) curves and (d–f) Dielectric constant–electric field curves, of the PLZT(001), PLZT(011) and PZT(111) thin films.

Table 1
Comparison of U_{stored}, U_{reco} and η values, defined from P–E loops as measured at 200 kV/cm, in the PLZT and PZT thin films with different orientations.

Sample	U_{stored} (J/cm^3)	U_{reco} (J/cm^3)	η % (= 100 × U_{reco}/U_{stored})
PLZT(001)	2.80	2.25	80.35
PLZT(011)	2.84	2.44	85.91
PLZT(111)	2.84	2.46	86.62
PZT(001)	5.48	1.01	18.52
PZT(011)	4.61	1.11	24.13
PZT(111)	4.21	1.12	26.67

Under the measurement condition (200 kV/cm), the corresponding maximum and remanent polarizations (P_m and P_r) are (27.6 and −0.3 μC/cm^2), (30.0 and 0.6 μC/cm^2) and (30.1 and 0.7 μC/cm^2) for the PLZT(001), PLZT(011) and PLZT(111) thin films, respectively. It is not much different in ($P_{max} - P_r$) values and therefore, the recoverable energy-storage density (U_{reco}) and energy-storage efficiency (η) are almost similar for these films, as shown in Fig. 3d. Meanwhile, the U_{stored} value in the PZT(001) film is much higher than that in the PZT(011) and PZT(111) films, due to the more square hysteresis loop in the PZT(001) film, but the but the U_{reco} value in the PZT(001) film is much smaller (see Fig. 5b). These results can be also seen in the Table 1.

The energy-storage performance of the PLZT thin films as a function of applied electric field (100–1000 kV/cm, 1 kHz and at room temperature) is presented in Fig. 6. As desired, the U_{stored} values increase with increasing electric field. The U_{stored} values are 13.91, 14.19 and 14.41 J/cm^3 for the PLZT(001), PLZT(011) and PLZT(111) films measured at 1000 kV/cm, respectively. In practical application, the larger η and/or U_{reco} values are also desires. With increase in the electric field, the U_{reco} values are increased while the η values are almost constant at approximately 86–88%. The U_{reco} values are 12.03, 12.51 and 12.74 J/cm^3 for the PLZT(001), PLZT(011) and PLZT(111) films measured at 1000 kV/cm, respectively. The high energy storage properties was also found in the antiferroelectric $Pb_{0.97}Y_{0.02}[(Zr_{0.6}Sn_{0.6})_{0.925}Ti_{0.075}]O_3$ thin film capacitors (U_{reco} = 14.6 J/cm^3 and η = 91.3% under an applied electric field of 1000 kV/cm) with the coexistence of the antiferroelectric and ferroelectric phases [18].

4. Conclusions

In summary, we have reported a correlation between the ferroelectric, energy-storage properties, and crystalline orientation of single crystal relaxor PLZT films, in comparison with the ferroelectric PZT films, epitaxially grown on STO substrates. The recoverable energy-storage density (U_{reco}) and energy-storage efficiency (η) of the PLZT films were much higher than those corresponding PZT films. Such remarkable enhancement maybe attributed to the antiferroelectric-like behavior in

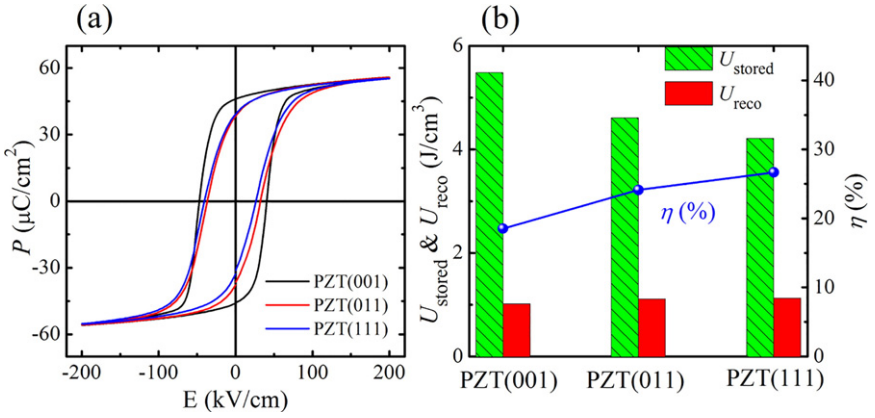

Fig. 5. (a) Ferroelectric hysteresis (P–E) loops and (b) the energy-stored per unit volume (U_{stored}), recoverable energy-storage density (U_{reco}) and energy-storage efficiency (η), of the PZT(001), PZT(011) and PZT(111) thin films. The PZT film thicknesses are about 500 nm.

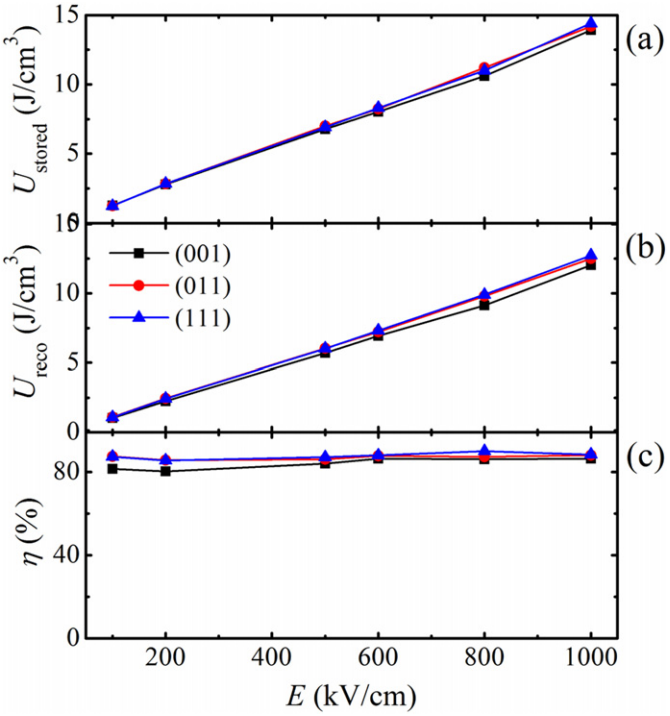

Fig. 6. Electric field dependence of (a) energy-stored per unit volume (U_{stored}), (b) recoverable energy-storage density (U_{reco}) and (c) energy-storage efficiency (η), of the PLZT(001), PLZT(011) and PZT(111) thin films.

the epitaxial PLZT films. Our results suggest that the (111)-oriented PLZT films are promising for the energy storage applications in high pulse capacitors.

Acknowledgements

The authors thank M. Smithers for performing the HRSEM experiments.

References

[1] M.D. Nguyen, E.P. Houwman, M. Dekkers, C.T.Q. Nguyen, H.N. Vu, G. Rijnders, Enhanced energy storage density and energy efficiency of epitaxial $Pb_{0.9}La_{0.1}(Zr_{0.52}Ti_{0.48})O_3$ relaxor-ferroelectric thin-films deposited on silicon by pulsed laser deposition, APL Mater. 4 (2016) 080701.
[2] N.H. Fletcher, A.D. Hilton, B.W. Ricketts, Optimization of energy storage density in ceramic capacitors, J. Phys. D. Appl. Phys. 29 (1996) 253–258.
[3] S. Patel, A. Chauhan, R. Vaish, Enhancing electrical energy storage density in anti-ferroelectric ceramics using ferroelastic domain switching, Mater. Res. Express 1 (2014), 045502.
[4] S. Tong, M. Narayanan, B. Ma, S. Liu, R.E. Koritala, U. Balachandran, D. Shi, Effect of lanthanum content and substrate strain on structural and electrical properties of lead lanthanum zirconate titanate thin films, Mater. Chem. Phys. 140 (2013) 427–430.
[5] A. Chauhan, S. Patel, R. Vaish, C.R. Bowen, Anti-ferroelectric ceramics for high energy density capacitors, Materials 8 (2015) 8009–8031.
[6] X. Hao, J. Zhai, X. Yao, Improved energy storage performance and fatigue endurance of Sr-doped $PbZrO_3$ antiferroelectric thin films, J. Am. Ceram. Soc. 92 (2009) 1133–1135.
[7] J. Ge, D. Remiens, X. Dong, Y. Chen, J. Costecalde, F. Gao, F. Cao, G. Wang, Enhancement of energy storage in epitaxial $PbZrO_3$ antiferroelectric films using strain engineering, Appl. Phys. Lett. 105 (2014) 112908.
[8] S.E. Young, J.Y. Zhang, W. Hong, X. Tan, Mechanical self-confinement to enhance energy storage density of antiferroelectric capacitors, J. Appl. Phys. 113 (2013), 054101.
[9] B. Peng, Q. Zhang, X. Li, T. Sun, H. Fan, S. Ke, M. Ye, Y. Wang, W. Lu, H. Niu, X. Zeng, H. Huang, Large energy storage density and high thermal stability in a highly textured (111)-oriented $Pb_{0.8}Ba_{0.2}ZrO_3$ relaxor thin film with the coexistence of antiferroelectric and ferroelectric phases, ACS Appl. Mater. Interfaces 7 (2015) 13512–13517.
[10] N. Ortega, A. Kumar, J.F. Scott, D.B. Chrisey, M. Tomazawa, S. Kumari, D.G.B. Diestra, R.S. Katiyar, Relaxor-ferroelectric superlattices: high energy density capacitors, J. Phys. Condens. Matter 24 (2012) 445901.
[11] X. Dai, Z. Xu, D. Viehland, Normal to relaxor ferroelectric transformations in lanthanum-modified tetragonal-structured lead zirconate titanate ceramics, J. Appl. Phys. 79 (1996) 1021–1026.
[12] X. Hao, Y. Wang, J. Yang, S. An, J. Xu, High energy-storage performance in $Pb_{0.91}La_{0.09}(Ti_{0.65}Zr_{0.35})O_3$ relaxor ferroelectric thin films, J. Appl. Phys. 112 (2012) 114111.
[13] Z. Hu, B. Ma, S. Liu, M. Narayanan, U. Balachandran, Relaxor behavior and energy storage performance of ferroelectric PLZT thin films with different Zr/Ti ratios, Ceram. Int. 40 (2014) 557–562.
[14] M.D. Nguyen, E. Houwman, M. Dekkers, H.N. Vu, G. Rijnders, A fast room-temperature poling process of piezoelectric $Pb(Zr_{0.45}Ti_{0.55})O_3$ thin films, Sci. Adv. Mater. 6 (2014) 243–251.
[15] M. Boota, E.P. Houwman, M. Dekkers, M.D. Nguyen, K.H. Vergeer, G. Lanzara, G. Koster, G. Rijnders, Properties of epitaxial, (001)- and (110)-oriented $(PbMg_{1/3}Nb_{2/3}O_3)_{2/3}$-$(PbTiO_3)_{1/3}$ films on silicon described by polarization rotation, Sci. Technol. Adv. Mater. 17 (2016) 45–57.
[16] M. Boota, E.P. Houwman, M. Dekkers, M. Nguyen, G. Rijnders, Epitaxial $Pb(Mg_{1/3}Nb_{2/3})O_3$-$PbTiO_3$ (67/33) thin films with large tunable self-bias field controlled by a $PbZr_{1-x}Ti_xO_3$ interfacial layer, Appl. Phys. Lett. 104 (2014) 182909.
[17] S.J. Kang, Y.H. Joung, Fatigue, retention and switching properties of PLZT(x/30/70) thin films with various La concentrations, J. Mater. Sci. 42 (2007) 7899–7905.
[18] C.W. Ahn, G. Amarsanaa, S.S. Won, S.A. Chae, D.S. Lee, I.W. Kim, Antiferroelectric thin-film capacitors with high energy-storage densities, low energy losses, and fast discharge times, ACS Appl. Mater. Interfaces 7 (2015) 26381–26386.